

*Full Length Research Paper*

# Convection flow of second grade fluid with uneven heat flux past an upright stretching flat surface

**\*Nassar Al-Sudais, Habib Al Qasabi and Abdulrahman Affan**

Department of Mathematics, Umm al-Qura University, Mecca, Saudi Arabia.

Accepted 23 June, 2014

In the present investigation, a numerical study of the flow and heat transfer analysis of viscoelastic second grade fluid due to heated, continuous stretching of a vertical sheet has been carried out. The stretching velocity is assumed to vary linearly with the distance measured from the leading edge. The surface heat flux is assumed to be varied in power of distance measured from the leading edge. The governing differential equations are transformed by introducing proper non-similarity variables and solved numerically using two different methods, namely, the local non-similarity method with second level of truncation and the implicit finite difference method for values of  $\xi (=Gr_x/Re_x^2)$  ranging from 0 to 10. The comparisons of the results obtained by the aforementioned methods are found in excellent agreement. Effects of the viscoelastic parameter,  $\lambda$  (Deborah number) on the skin-friction and the heat transfer coefficients have been shown graphically for the fluid with Prandtl number equal to 0.7, 7.03 and 15.0.

**Key words:** Mixed convection, second grade fluid, stretching flat surface, variable surface heat flux.

## INTRODUCTION

Recently, Mushtaq et al. (2007) explored the effects of thermal buoyancy on flow of a viscoelastic second grade fluid past a vertical, continuous stretching sheet of which the velocity and temperature distributions are assumed to vary according to a power-law form. In the present investigation we have analyzed the mixed convection flow of the same fluid along a continuously stretched vertically placed heated surface subject to non-uniform surface heat flux.

In actual practice, the flow of viscous incompressible fluid over a continuous material moving through a quiescent fluid is induced by the movement of the solid material and by thermal buoyancy. Therefore, these two mechanisms, surface motion and buoyancy force, will determine the momentum and thermal transport processes. The thermal buoyancy force arising due to the

heating or cooling of a continuously moving surface may alter significantly the flow and thermal fields and thereby the heat transfer behavior in the manufacturing process. The literature survey shows that, a continuously moving surface through a quiescent medium has many engineering applications; such as hot rolling, wire drawing, spinning of filaments, metal extrusion, crystal growing, continuous casting, glass fiber production, and paper production (Altan et al., 1979; Fisher, 1976; Tadmor and Klein, 1970). On the other hand, Karwe and Jaluria (1988, 1991) showed that the thermal buoyancy effects are more prominent when the plate moves vertically, that is, aligned with gravity, than when it is horizontal. In their analysis, they treated the mixed convection flow of aforementioned fluid over a continuous plate moving at a uniform speed, which may have applications in material processes, such as hot rolling, extrusion, and drawing. The numerical solution for the boundary layer flow was first presented by Sakiadis (1961). Later on, Magyari et al. (2001) and Magyari and

\*Corresponding author. E-mail: [sudias2011@yahoo.com](mailto:sudias2011@yahoo.com)

Keller (2000) reported numerical solution for rapidly decreasing velocity using self-similar method and the analytical solution for permeable surface moving with a decreasing velocity. Chen and Strobel (1980) dealt with the problem of combined forced and free convection flow of viscous incompressible fluid in boundary layers adjacent to a continuous horizontal sheet maintained at a constant temperature and moving with a constant velocity. Ingham (1986) investigated the existence of the solutions for the free convection boundary-layer flow of viscous fluid near a continuously moving vertical plate with temperature inversely proportional to the distance up the plate. Ali and Al-Yousef (1998) have investigated the problem of laminar mixed convection flow adjacent to a uniformly moving permeable vertical plate. Also, an analysis of mixed convection heat transfer from a vertical, continuously stretching sheet has been presented later on by Chen (1998). All the previous investigations were confined to the case of Newtonian fluid only.

In recent years non-Newtonian fluids, such as, Walter's fluid (Walters, 1962) or the viscoelastic second grade fluid, have become increasingly important from the point of industrial applications; for example, in certain polymer processing, one deals with flow of a non-Newtonian fluid over a stretching surface; since, these fluids show viscoelastic behavior, meaning that very short part of the history of the deformation gradient has an effect on the stress. In an incompressible fluid of differential type, apart from a constitutively indeterminate pressure, the stress is just a function of its velocity gradient and some number of its higher-time derivatives. These fluids do not exhibit the phenomenon of stress relaxation which means that with the instantaneous cessation of all local motion, the stress becomes pure pressure. Issues concerning the status of second grade fluid were discussed by Dunn and Rajagopal (1995).

Steady flow of a viscoelastic second-order fluid past a stretching sheet was investigated by Rajagopal et al. (1984). Bhattacharyya et al. (1998) studied the temperature distribution in the steady boundary layer flow of a second-order fluid past a stretching surface. Later, Chen et al. (1990) studied the flow and heat transfer in the boundary layer of a viscoelastic second grade fluid over a stretching surface subject to either constant temperature or uniform heat flux.

In the present investigation, we have analyzed the mixed convection flow of viscoelastic second grade, fluid along a heated and continuously moving surface subject to non-uniform surface heat flux. We further assume that the surface velocity is proportional to  $x$  and the wall heat flux is proportional to  $x^m$ , where  $x$  measures the distance from the leading edge of the stretched surface. The dimensionless boundary layer equations that govern the flow and heat transfer are transformed to local non-similarity equations using suitable transformations which are then solved numerically applying (i) the local non-similarity method as well as (ii) the implicit finite

difference method. The numerical results thus obtained are presented in terms of local skin-friction and local Nusselt number for different values of the physical parameters, such as, the viscoelastic parameter,  $\lambda$  (also known as the Deborah number) and for Prandtl number,  $Pr$ , choosing the values of  $\xi$  within the range of 0 to 10. Conjugate effects of the viscoelastic parameter  $\lambda$  as well as the local mixed convection parameter  $\xi$  on the velocity and temperature field have also been shown graphically.

**FORMULATION OF THE PROBLEM**

We consider a steady two-dimensional mixed convection flow of a viscoelastic second grade fluid along a vertically stretching flat surface subject to variable heat-flux proportional to  $x^m$ , that is,  $q_w(x)=q_0(x/L)^m$ , where  $x$  measures the distance from the leading edge of the plate and  $m$  is a real number. The flow configuration is shown in Figure 1, in which  $y$  measures the distance from the surface in the direction normal to  $x$ . The ambient temperature is assumed to be,  $T_\infty$ , constant. Here  $u$  and  $v$  are the  $x$ - and  $y$ -components of the fluid velocity and  $T$  being the temperature of the fluid in the boundary layer region. Finally, the stretching velocity is assumed to be a linear function of  $x$ , that is,  $U_w(x)=U_0(x/L)$ . Under the usual Boussinesq approximation, the governing dimensionless boundary layer equations for the conservation of mass, momentum and energy are given in Equations 1 to 3:

$$\frac{\partial U}{\partial X} + \frac{\partial V}{\partial Y} = 0 \tag{1}$$

$$U \frac{\partial U}{\partial X} + V \frac{\partial U}{\partial Y} = \frac{\partial}{\partial X} \left( \frac{\partial^2 U}{\partial Y^2} \right) + \frac{\partial}{\partial Y} \left( \frac{\partial^2 U}{\partial X \partial Y} \right) + \frac{\partial}{\partial Y} \left( \frac{\partial^2 U}{\partial Y^2} \right) + Ri \Theta \tag{2}$$

$$U \frac{\partial \Theta}{\partial X} + V \frac{\partial \Theta}{\partial Y} = \frac{1}{Pr} \frac{\partial^2 \Theta}{\partial Y^2} \tag{3}$$

$$\frac{\partial \Theta}{\partial X} = 0 \tag{4}$$

$$U = X, \quad V = 0, \quad \frac{\partial \Theta}{\partial Y} = -X \quad \text{at } Y = 0 \\ U \rightarrow 0, \quad \Theta \rightarrow 0 \quad \text{as } Y \rightarrow \infty \tag{5}$$

The aforementioned dimensionless equations are being obtained by introducing the following dependent and independent dimensionless quantities;

$$X = \frac{x}{L}, \quad Y = \frac{y}{L} Re_L^{1/2}, \quad Ri = \frac{Gr_L}{Re_L^{5/2}} \\ U(X, Y) = \frac{u}{U_0}, \quad V(X, Y) = \frac{L}{v_{Re}^{1/2}} v, \quad \Theta(X, Y) = \frac{k Re_L^{1/2}}{L q_0} (T - T_\infty) \tag{6} \\ U(x) = U_0 (x/L), \quad q_w(x) = q_0 (x/L)^m$$

Where,  $u, v, T$  are the dependent variables and  $\Theta$  is dimensionless temperature at the surface of the plate. The dimensional  $U_0$  and  $q_0$  are prescribed constants,  $m$  is the exponent

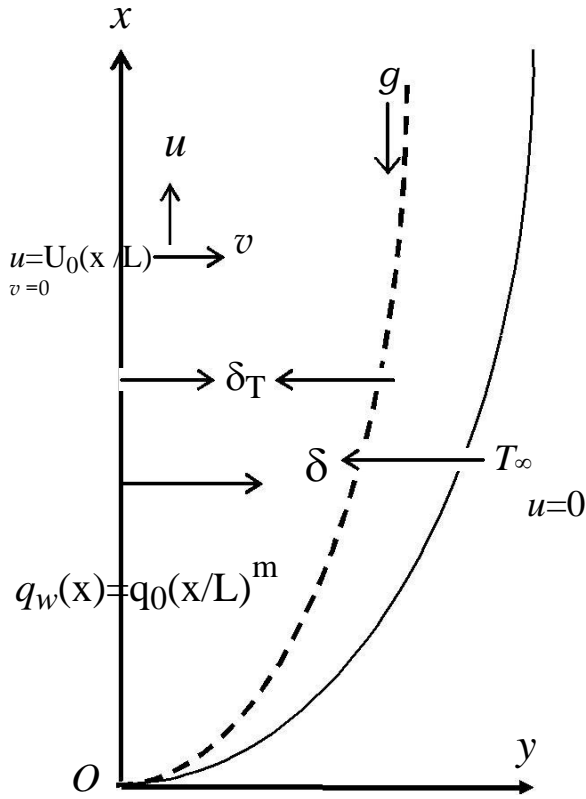


Figure 1. The flow configuration and the coordinate system.

and  $T_\infty$  is the temperature of the ambient fluid. Further,  $Ri$  is the Richardson number together with Equation 7 as the Reynolds number and the modified Grashof number for the heat-flux case. Further, in Equation 2,  $\lambda = KRe/L^2$  denotes the viscoelastic parameter (or Deborah number):

$$Re = UL/\nu, Gr = g\beta q L^4/k\nu^2 \quad (7)$$

It can be seen that Equations 1 to 3 admit self-similar solution and hence we may introduce the following free group of transformations:

$$\eta = Y, \quad \xi = RiX^{m-1}, \quad \psi = Xf(\eta, \xi), \quad \Theta = X^m\theta(\eta, \xi) \quad (8)$$

Introducing the new dimensionless variables given in Equation 8, Equations 2 and 3 can be written in the following dimensionless form:

$$\theta_\eta = \frac{1}{r} e^{-r\xi} M \left( \begin{matrix} -r\xi \\ s-2, s+1, -s \end{matrix} \right) \left[ sM \left( \begin{matrix} -r\xi \\ s-2, s+1, -s \end{matrix} \right) \right]^{-1} \quad (18)$$

Where:

$$M(a, b, z) = 1 + \sum_{n=1}^{\infty} \frac{(a)_n}{(b)_n} \frac{z^n}{n!} \quad (19)$$

is the Kummer's function, and:

$$f''' + ff'' - f^2 + \lambda(2ff''' - (f'')^2 - ff^{iv}) + \xi\theta = (m-1)\xi \left[ f' \frac{\partial f'}{\partial \xi} - f'' \frac{\partial f}{\partial \xi} - \lambda \left( f' \frac{\partial f'''}{\partial \xi} + f'''' \frac{\partial f}{\partial \xi} - f'' \frac{\partial f''}{\partial \xi} - f^{iv} \frac{\partial f}{\partial \xi} \right) \right] \quad (9)$$

$$\frac{1}{Pr} \theta'' + f\theta' - m\theta f' = (m-1)\xi \left( f' \frac{\partial \theta}{\partial \xi} - \theta' \frac{\partial f}{\partial \xi} \right) \quad (10)$$

With the aforementioned transformation corresponding boundary conditions, Equations 4 and 5 will turn into:

$$f(0, \xi) = 0, \quad f'(0, \xi) = 1, \quad f'(\infty, \xi) = 0 \quad (11)$$

$$\theta(0, \xi) = -1, \quad \theta(\infty, \xi) = 0 \quad (12)$$

Where, a prime denotes differentiation with respect to  $\eta$ .

In the case of local mixed convection parameter  $\xi = 0$  and surface heat flux exponent  $m = 2$ , Equations 9 to 12 will take the following form:

$$f''' + ff'' - f^2 + \lambda(2ff''' - (f'')^2 - ff^{iv}) = 0 \quad (13)$$

$$\frac{1}{Pr} \theta'' + f\theta' - 2\theta f' = 0 \quad (14)$$

$$f(0, \xi) = 0, \quad f'(0, \xi) = 1, \quad f'(\infty, \xi) = 0 \quad (15)$$

$$\theta(0, \xi) = -1, \quad \theta(\infty, \xi) = 0 \quad (16)$$

Equations 13 to 16 have become well-known equations that govern the flow of second grade viscoelastic fluid and heat transfer in the boundary layer region along a stretching sheet with power law surface heat flux. A similar problem had been investigated by Liu (2005).

Following the methodology used by Liu (2005), the analytical solutions of Equations 13 to 16 are obtained as shown:

$$f(\eta) = \frac{1}{r} \left( 1 - e^{-r\eta} \right) \quad (17)$$

$$(a)_n = a(a+1)(a+2)\dots(a+n-1) \quad (20)$$

$$r = \frac{1}{\sqrt{1+\lambda}}, \quad s = Pr(1+\lambda) \quad (21)$$

The skin-friction coefficient,  $f''(0)$ , and the heat transfer coefficient,  $1/\theta(0)$ , are found to be:

$$r = \frac{1}{\sqrt{1+\lambda}}, \quad s = \text{Pr}(1+\lambda) \tag{22}$$

$$1/\theta(0) = \left[ sM(s-2, s+1, -s) - s(s-2)M(s-1, s+2, -s) / (s+1) \right] / \left[ \sqrt{1+\lambda}M(s-2, s+1, -s) \right] \tag{23}$$

The numerical values of  $1/\theta(0)$  obtained using Equation 23 and also obtained by the implicit finite difference method (discussed subsequently) at selected values of viscoelastic parameter  $\lambda$  and Prandtl number  $Pr$  are entered in Table 2. From this table, it can be seen that the present numerical values are in excellent agreement with that of Liu (2005); since, the maximum difference between these two results is less than 0.5%.

**SOLUTION METHODOLOGIES**

As a first attempt, we employ the local non-similarity method of Sparrow and Yu (1971) in finding the solutions of Equations 9 to 12 by treating the local variable  $\xi$  as the non-similar parameter. Solutions for all  $\xi$  are then obtained by the implicit finite difference method together with Keller-box elimination technique (Keller, 1978) as well. Short description of the aforementioned methods will be provided subsequently.

**Local non-similarity method**

With the exception of a few specially proposed boundary conditions (Sparrow and Gregg, 1958; Semenov, 1984), the vertical free convection boundary layer problems are normally locally non-similar. The local similar method reduces the coupled partial differential equations into a set of nonlinear ordinary differential equations to be solved numerically. However, the error introduced by this technique cannot be easily estimated. Sparrow et al. (1970) introduced the local non-similar method to improve this concept. However, like the local non-similar method, this technique is locally autonomous. Solutions at any specified stream wise station can be obtained without first obtaining upstream solutions. Keller and Yang (1972) employed a Görtler-type series to study the free convection boundary-layer flow along a non-isothermal vertical plate assuming that the wall temperature can be represented by a power series in the stream wise coordinate. Later, Kao et al. (1977) proposed the method of strained coordinates for the computation of the wall heat transfer parameter for a plate with an arbitrary prescribed surface temperature. In this method, the coordinate along the plate was transformed by using an integral function of the specified wall temperature so that the problem can be solved with any specified surface conditions. The non-similar solution can then be obtained for the local similarity solution by determining an approximate wedge parameter in such a way that the local similarity results give a value that would be obtained if one considers the local non-similarity solution method. Following this technique, the determination of the approximate wedge parameter involves an estimation and iterative procedure. Further, Yang et al. (1982) proposed an alternative method to evaluate the surface heat transfer rate and the wall shear stress for free convection boundary-layer flow considered by Kao et al. (1977) using a Merk-type series solution (Merk, 1959). The governing coupled partial differential equations in Kao et al. (1977) were transformed into a sequence of coupled ordinary differential equations which were then solved numerically by a fourth-order Runge-Kutta scheme with an incorporated least-squares convergence criteria for the zeroth-order solution and with the Newton-Raphson iteration scheme for higher-order solutions.

This section is concerned with the local non similarity method initiated by Sparrow and Yu (1971) and Minkowycz and Sparrow (1978) which has later been applied by many investigators such as Mushtaq et al. (2007), Hossain and Takhar (1996), Hossain et al. (1994) and Chen (1988). Formulation of the system of equations for the present local non similarity model, with reference to the present problem, will be demonstrated subsequently.

**First level of truncation**

At the first level of truncation, the terms of the form  $\xi \partial(\ ) / \partial \xi$  are deleted from the right hand side of Equations 9 and 10 (Sparrow and Yu, 1978) to yield the following system of equations:

$$f''' + ff'' - f'^2 + \lambda(2ff''' - (f'')^2 - ff^{iv}) + \xi\theta = 0 \tag{24}$$

$$\frac{1}{Pr} \theta'' + f\theta' - m\theta f' = 0 \tag{25}$$

$$f(0, \xi) = 0, f'(0, \xi) = 1, f'(\infty, \xi) = 0 \tag{26}$$

$$\theta(0, \xi) = -1, \theta(\infty, \xi) = 0 \tag{27}$$

It can be seen that Equations 24 and 25 can be regarded as a system of ordinary differential equations for the functions  $f$  and  $\theta$  with  $\xi$  as a parameter for a given Prandtl number  $Pr$  and a viscoelastic parameter  $\lambda$ .

**Second level of truncation**

To find the higher level of truncation, we introduce the following functions:

$$g(\eta, \xi) = \frac{\partial f}{\partial \xi}, \quad \phi(\eta, \xi) = \frac{\partial \theta}{\partial \xi} \tag{28}$$

For the second level, the governing Equations 9 and 10 are retained in full as:

$$f''' + ff'' - f'^2 + \lambda(2ff''' - (f'')^2 - ff^{iv}) + \xi\theta = 0 \tag{29}$$

$$= \left[ \begin{matrix} m-1 \xi | f' g & -f' g' - \lambda & f' g''' + & f'' g' - f'' g'' - f g \\ & & & iv \end{matrix} \right] \tag{30}$$

$$\frac{1}{Pr} \theta'' + f\theta' - m\theta f' = \left( \begin{matrix} m-1 \xi & f' \phi - \theta' g \end{matrix} \right) \tag{31}$$

$$\theta(0, \xi) = -1, \theta(\infty, \xi) = 0 \tag{32}$$

by taking derivatives of Equations 29 to 32 with respect to  $\xi$ . This leads to:

The equations and boundary condition for  $g$  and  $\phi$  can be devised

$$g''' + fg'' + mf'g' - (m+1)fg'' + \lambda \left[ m+1 fg'' + (m+1) f''g' - (m+1) f'g''' \right] - \frac{iv}{g} \left[ \frac{iv}{g} + \theta + \xi \phi \right] = 0 \tag{33}$$

$$\frac{1}{Pr} \phi' + f\phi + mg\theta' - mg'\theta - (2m-1)f'\phi = (m-1)\xi [g'\phi - \phi g] \tag{34}$$

$$g(0, \xi) = 0, g'(0, \xi) = 0, g'(\infty, \xi) = 0 \tag{35}$$

$$\phi(0, \xi) = 0, \phi(\infty, \xi) = 0 \tag{36}$$

At this level of truncation,  $\partial g/\partial \xi$  and  $\partial \phi/\partial \xi$  and their derivatives with respect to  $\eta$  are neglected. This was first considered by Chen (2000) to obtain more accurate results. Considering the present scheme, solutions for  $f, g, \theta$  and  $\phi$  are obtained using the Natschein-Swigert iteration technique. The required missing values of  $f''(0, \xi)$  and  $\theta(0, \xi)$  are obtained to measure the values of local skin-friction coefficient,  $Cf_{Re_x}^{1/2}$ , and local heat transfer coefficient,  $Nu_{Re_x}^{-1/2}$ . The numerical values obtained for these quantities are depicted in Table 1 and compared with the solution obtained by the implicit finite difference method discussed subsequently and an excellent agreement is achieved.

**Implicit finite difference solutions**

The governing Equations 9 and 10 are revisited and the numerical solution is initiated using Keller Box scheme. We recast these equations into a set of simultaneous equations by introducing the variables  $U, V, W$  and  $P$ :

$$f' = F, F' = G, G' = H, \theta = P \tag{37}$$

$$G' + fG - F^2 + \lambda \left[ 2FH - G^2 - fH' \right] + \xi \theta = (m-1)\xi \left[ F \frac{\partial F}{\partial \xi} - G \frac{\partial f}{\partial \xi} - \lambda \left( F \frac{\partial H}{\partial \xi} + H \frac{\partial F}{\partial \xi} - G \frac{\partial G}{\partial \xi} - H' \frac{\partial f}{\partial \xi} \right) \right] \tag{38}$$

$$\frac{1}{Pr} P' + fP - m\theta F = (m-1)\xi \left( F \frac{\partial \theta}{\partial \xi} - P \frac{\partial f}{\partial \xi} \right) \tag{39}$$

$$f(0, \xi) = 0, F(0, \xi) = 1, P(0, \xi) = -1 \tag{40}$$

$$F(\infty, \xi) = 0, \theta(\infty, \xi) = 0 \tag{41}$$

We now place a net on the  $(\eta, \xi)$  plane defined by:

$$\eta = 0, \eta = \eta_{ii-1} + h_i, \quad i = 1, 2, 3, \dots, M$$

Which are then expressed in finite difference form by approximating the functions and their derivatives in terms of the central differences in both coordinate directions. Denoting the mesh points in the  $(\eta, \xi)$  plane by  $\eta_i$  and  $\xi_j$ , where  $i = 1, 2, 3, \dots, M$  and  $j = 1, 2, 3, \dots, N$ , central difference approximations are made such that the equations involving  $\xi$  explicitly, are centred at  $(\eta_{i-1/2}, \xi_{j-1/2})$  and the remainder at  $(\eta_{i+1/2}, \xi_j)$ , where  $\eta_{i-1/2} = (\eta_i + \eta_{i-1})/2$ , etc. This results in a set of nonlinear difference equations for the unknowns at  $\eta_i$  in terms of their values at  $\eta_{i-1}$ . These equations are then linearised by the Newton's quasi-linearization technique and are solved using a block-tridiagonal algorithm, taking as the initial iteration of the converged solution,  $\eta_i = \eta_{i-1}$ . Now to initiate the process at  $\eta = 0$ , we first provide guess profiles for all five variables (arising the reduction to the first order form) and use the Keller box method to solve the governing ordinary differential equations. Having obtained the lower stagnation point solution it is possible to march step by step along the boundary layer. For a given value of  $\eta$ , the iterative procedure is stopped when the difference in computing the velocity and the temperature in the next iteration is less than  $10^{-5}$ , that is, when  $|\delta f^i| \leq 10^{-5}$ , where the superscript denotes the iteration number. The computations were not performed using a uniform grid in the  $\xi$  direction, but a non-uniform grid was used and defined by  $\eta_i = \sinh((i-1)/p)$ , with  $i = 1, 2, \dots, 301$  and  $p = 100$ .

**RESULTS AND DISCUSSION**

In the present investigation, two distinct methodologies were used to obtain the solution of the problem on mixed convection flow of viscoelastic second grade fluid along a non-isothermal stretched vertical surface. The physical

parameters that control the flow and heat transfer are the Prandtl number,  $Pr$ , the viscoelastic parameter,  $\lambda$ , and the local Richardson number (also termed as the local mixed-convection parameter),  $\xi$ . Due to the presence of

this local variable,  $\xi$ , the governing equations for the flow and heat transfer appeared as non-similarity equations.

For values of,  $\xi$ , in the range of 0 to 10, the solutions are obtained by employing the local non similarity method

and the implicit finite difference method. Once the functions  $f$  and  $\theta$  and their derivatives are known, the

important physical quantities, such as, the wall shear stress and the surface heat flux can be determined easily. The wall shear is expressed in terms of the local skin friction coefficient as:

$$C_{fx} = 2\tau_w(x) / \rho(U_w(x))^2 \tag{42}$$

**Table 1.** Numerical values of  $f(0, \xi)$  and  $1/\theta(0, \xi)$  obtained by local non-similarity method and implicit finite difference method against  $\xi$  when  $Pr = 0.70$ ,  $\lambda = 1.0$  and  $m = 2.0$ .

$\xi$	$f(0, \xi)$		$1/\theta(0, \xi)$	
	LNS	FDM	LNS	FDM
0.00	-1.43788	-1.43764	1.02730	1.02730
0.25	-1.23718	-1.22929	1.06312	1.06263
0.50	-1.08240	-1.08563	1.08836	1.08674
0.75	-0.95084	-0.94250	1.10858	1.10619
1.00	-0.83465	-0.83850	1.12573	1.12274
1.25	-0.72974	-0.72161	1.14074	1.13727
1.50	-0.63357	-0.63629	1.15415	1.15029
1.75	-0.54446	-0.53821	1.16632	1.16212
2.00	-0.46119	-0.46150	1.17749	1.17299
2.50	-0.30882	-0.30727	1.19748	1.19247
3.00	-0.17144	-0.16924	1.21504	1.20961
4.00	0.07035	0.07249	1.24503	1.23893
5.00	0.28018	0.28207	1.27021	1.26361
6.00	0.46685	0.46834	1.29203	1.28507
7.00	0.63584	0.63673	1.31134	1.30408
8.00	0.79079	0.79096	1.32871	1.32116
9.00	0.93428	0.93366	1.34451	1.33668
10.00	1.06555	1.06544	1.35551	1.35081

And the local Nusselt number as:

$$N_{ux} = q_w(x) x / k(T_w - T_\infty) \tag{43}$$

Where:

$$\tau_w(x) = \mu \left( \frac{\partial u}{\partial y} \right)_{y=0} + \kappa \left[ u \frac{\partial^2 u}{\partial x \partial y} + v \frac{\partial^2 u}{\partial y^2} + 2 \frac{\partial u}{\partial x} \frac{\partial u}{\partial y} \right]_{y=0} \tag{44}$$

And:

$$(T_w - T_\infty) / (T_w - T_\infty) = \theta(\eta, \xi) / \theta(0, \xi) \tag{45}$$

Using Equations 42 and 43, we can express the local skin-friction,  $C_{fx}$  as:

$$Re_x^{1/2} C_{fx} = 2(1 + 3\lambda) f''(0, \xi) \tag{46}$$

And the local Nusselt number as:

$$Re_x^{-1/2} N_{ux} = 1/\theta(0, \xi). \tag{47}$$

The results are obtained in terms of local skin-friction and local Nusselt number against the mixed convection parameter  $\xi$  using the relations given in Equations 46 and 47.

Table 2 shows the comparison of analytical values of the local Nusselt number,  $Nu_x$ , using the methodology employed by Liu (2005) and those of present work obtained by the implicit finite difference method at selected values of  $\lambda$  and  $Pr$  when local mixed convection parameter  $\xi = 0$  and surface heat flux exponent  $m = 2$ .

The numerical values of the local skin-friction coefficient,  $f''(0, \xi)$ , and local heat transfer coefficient,  $1/\theta(0, \xi)$  for  $Pr = 0.70$ ,  $\lambda = 1.0$  and  $m = 2.0$  obtained against local mixed convection parameter  $\xi$  in  $[0.0, 10.0]$  by the aforementioned methods are entered in Table 2. The results thus found are almost identical for all  $\xi$  in  $[0.0, 10.0]$ . Henceforth, the results discussed in the following paragraphs are due to implicit finite difference method only.

As a benchmark, the solution of Equations 13 to 16 obtained by the present authors is compared with the one obtained by Chen et al. (1990) in Figure 2a and b as our special case when  $\lambda = 0$  and  $m = 1$ . It can be seen that these two results are in complete harmony with those presented in Chen et al. (1990).

### Effect of physical parameters on skin-friction and Nusselt number

Numerical values of the local skin-friction coefficient as well as local heat transfer coefficient are depicted, respectively, in Figure 3a and b against  $\xi$ , while values of  $Pr$  equal to 0.70, 7.03 and 15.0 and that of  $\lambda = 1$  and  $m =$

**Table 2.** Comparison of analytical (Liu et al., 2005) and numerical values (present work) at selected values of  $\lambda$  and  $Pr$  when  $\xi = 0$  and  $m = 2$ .

$\lambda$	$Pr$	$1/\theta(0)$	
		Liu (2005)	Present
0.0	0.70	1.06932	1.06933
	7.03	3.98056	3.98047
	15.00	5.93201	5.93169
1.0	0.70	1.15164	1.15126
	7.03	4.05531	3.89170
	15.00	6.00567	5.83579
2.0	0.70	1.18707	1.18264
	7.03	4.08805	3.60160
	15.00	6.03805	5.65077

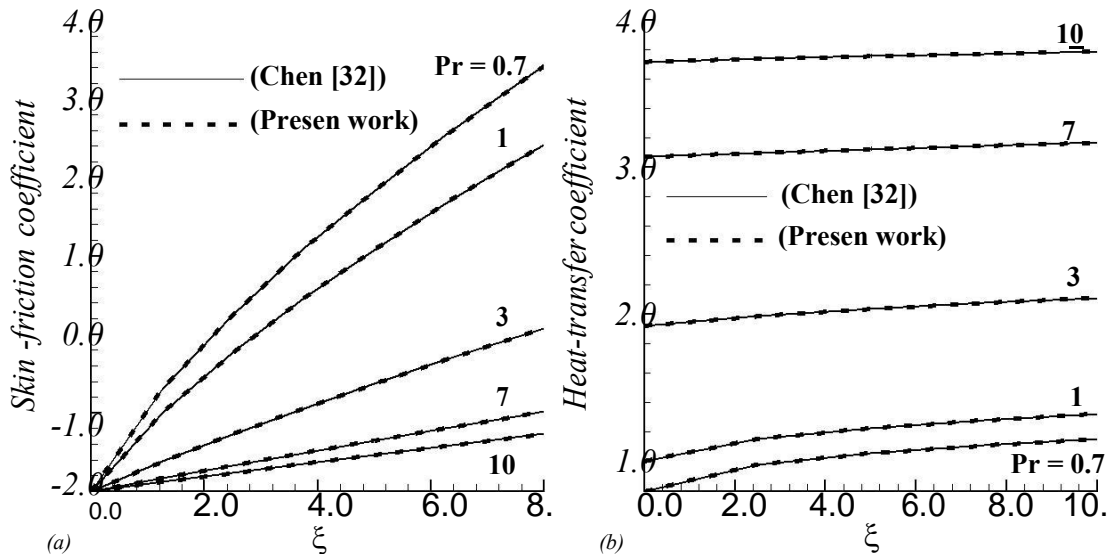


**Figure 2.** Numerical values of (a)  $Re_x^{1/2} Cf_x/2$ , local skin-friction coefficient and (b)  $Re_x^{-1/2} Nu_x$ , local heat transfer coefficient against  $\xi$  at selected values of  $Pr$  while  $\lambda = 0$  and  $m = 1$ .

2.0. It may be observed that, for the given value of  $Pr$ , owing to increase in the value of local mixed convection parameter  $\xi$ , there is increase in both the local skin-friction  $Re_x^{1/2} Cf_x/2$  and the local heat transfer coefficient,  $Re_x^{-1/2} Nu_x$ , which is expected, since in the downstream region the flow is dominated by the buoyancy force rather than the stretching rate of the plate. We further observe that increase in the value of  $Re_x^{1/2} Cf_x/2$  is faster than that of  $Re_x^{-1/2} Nu_x$  at a given value of  $Pr$ . From the same figure it may be noticed that, for an increase in  $Pr$ , the value of the local skin-friction coefficient,  $Re_x^{1/2} Cf_x/2$ , decreases where as there is increase in the value of the local heat transfer coefficient,  $Re_x^{-1/2} Nu_x$ . Now, we discuss the effect of the Deborah number ( $\lambda$ ) on the local skin-friction

coefficient,  $Re_x^{1/2} Cf_x/2$  and the local heat transfer coefficient,  $Re_x^{-1/2} Nu_x$ . Numerical values of the local skin-friction coefficient,  $Re_x^{1/2} Cf_x/2$  and the local heat transfer coefficient,  $Re_x^{-1/2} Nu_x$  are depicted, respectively, in Figure 4a and b for values of  $\lambda$  equal to 0.0, 1.0 and 2.0 while the fluid's  $Pr$  is 7.03 and surface heat flux exponent  $m$  is 2.0 for  $\xi \in [0, 10]$ . From these figure one may observe that very near the leading edge there is decrease in the values of the local skin-friction coefficient and local heat transfer coefficient, owing to increase in  $\lambda$ . On the other hand, in the downstream-regime, values of both these physical quantities increase with the increase in  $\lambda$ .

This is expected, since in the downstream region the affect of the elastic property of the fluid get suppressed

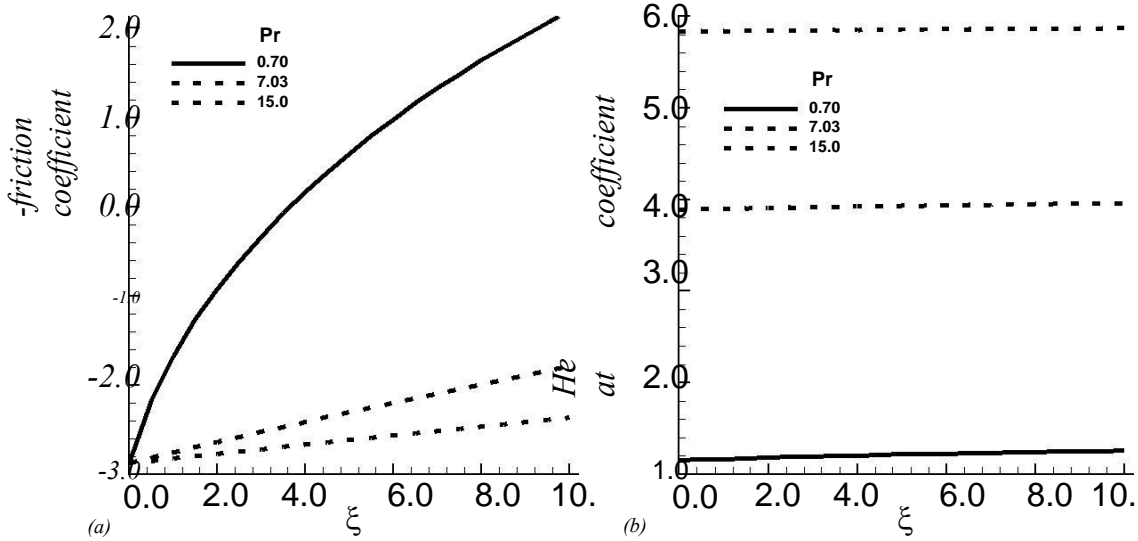


**Figure 3.** Variation of (a) local skin-friction coefficient and (b) local heat transfer coefficient with  $\xi$  at selected values of Prandtl number  $Pr$  when viscoelastic parameter  $\lambda = 1$  and surface heat flux exponent  $m = 2$ .

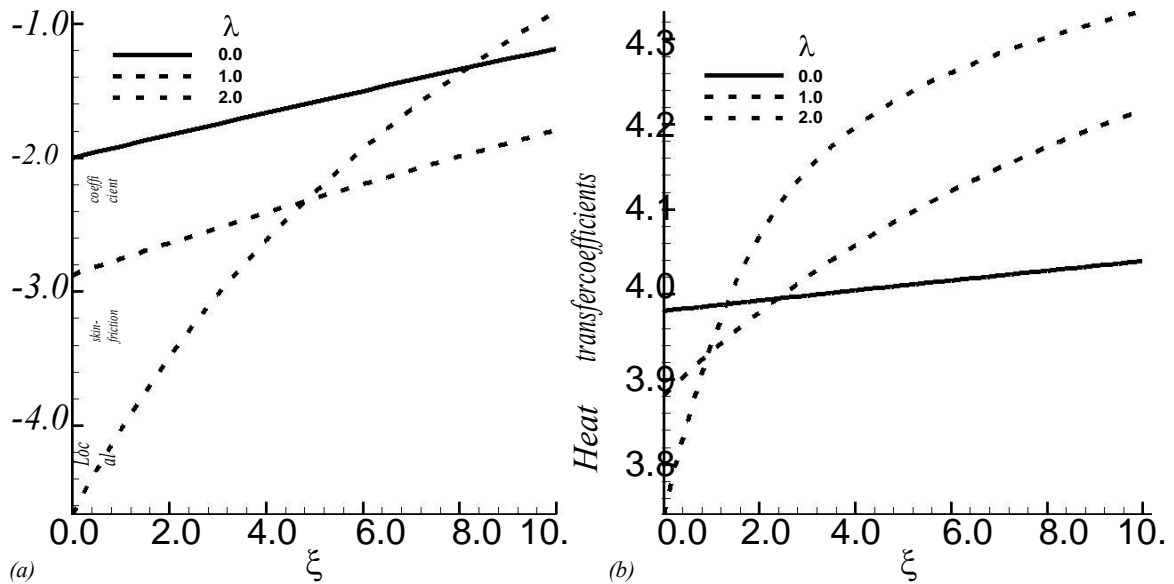


**Figure 4.** Variation of (a) local skin-friction coefficient and (b) local heat transfer coefficient with  $\xi$  at selected values of viscoelastic parameter  $\lambda$  when Prandtl number  $Pr = 7.03$  and surface heat flux exponent  $m = 2$ .

by the buoyancy force whereas it is strong near the leading edge.

Figure 5a and b illustrate the effect of varying surface heat flux exponent,  $m$ , on the local skin-friction coefficient,  $Re_x^{1/2} Cf_x/2$ , and the local heat transfer coefficient,  $Re_x^{-1/2} Nu_x$ , against local mixed convection parameter  $\xi \in [0, 10]$  for  $\lambda = 1$  and the  $Pr = 7.03$ . It can be noticed from Figure 5a that owing to increase in the surface heat flux exponent,  $m$ , the local skin-friction coefficient increases and the rate of increase first

decreases and then increases, away from the leading edge. It may be observed from Figure 5b that, owing to increase in the surface heat flux exponent,  $m$ , the local heat transfer coefficient increases near the leading edge. From these figure, it can be noticed that both the local skin-friction coefficient,  $Re_x^{1/2} Cf_x/2$ , and the local heat transfer coefficient,  $Re_x^{-1/2} Nu_x$  increases as moving away from the leading edge but increase in local skin-friction coefficient is higher than that of the local heat transfer coefficient.



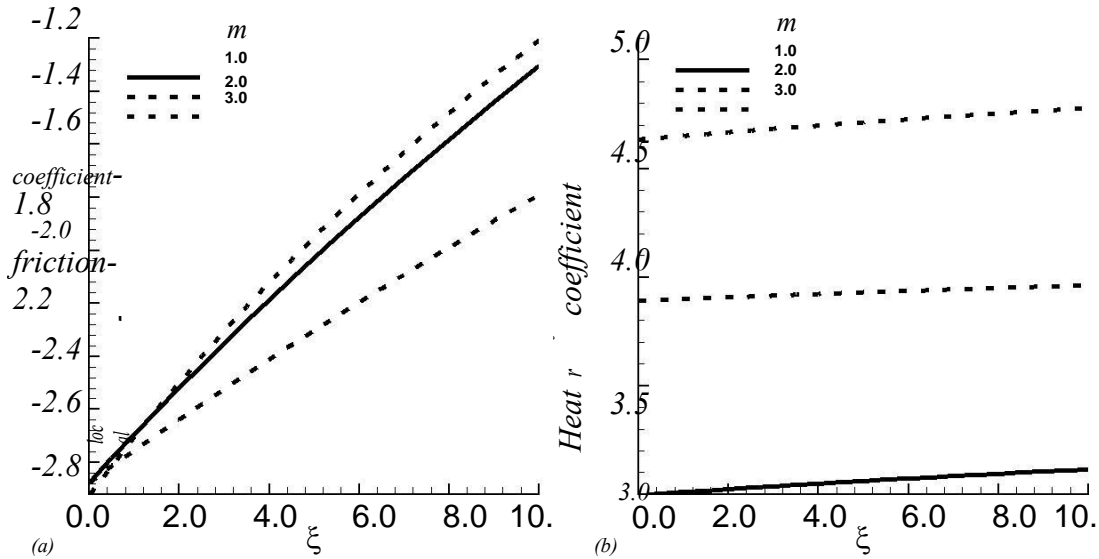


**Figure 5.** Variation of (a) local skin-friction coefficient and (b) local heat transfer coefficient with  $\xi$  at selected values of surface heat flux exponent  $m$  when Prandtl number  $Pr = 7.03$  and viscoelastic parameter  $\lambda = 1$ .

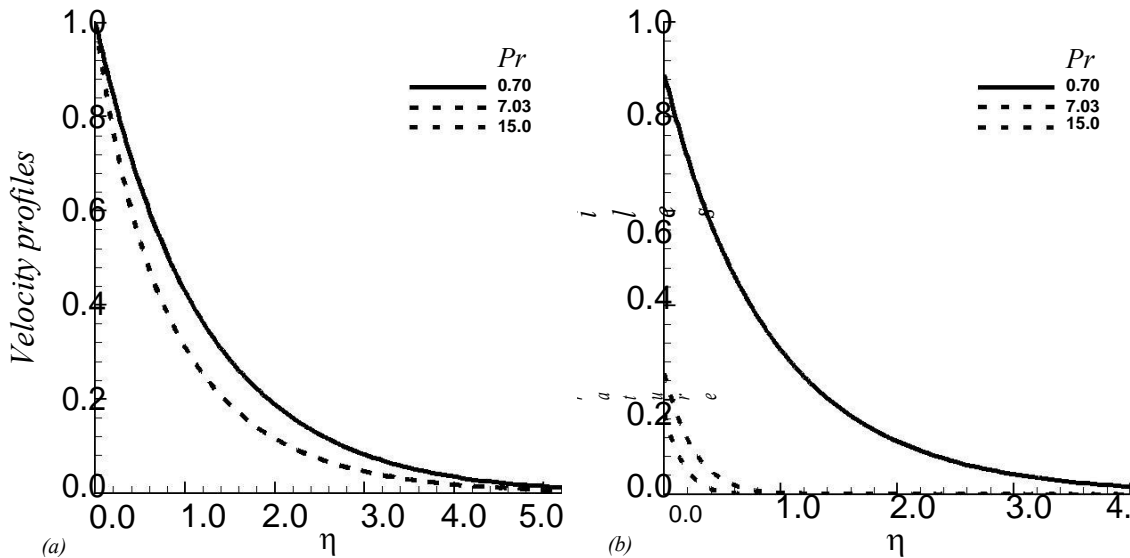


**Figure 6.** Variation of (a) velocity profiles and (b) temperature profiles against  $\eta$  for selected values of the Prandtl number  $Pr$  when viscoelastic parameter  $\lambda = 1.0$ , surface heat flux exponent  $m = 2$  and local mixed convection parameter  $\xi = 1$ .

**Effect of physical parameters on velocity and temperature profiles**

Dimensionless velocity and temperature profiles are shown in Figure 6a and b, respectively, against  $\eta$  for  $Pr = 0.70, 7.03$  and  $15.0$  while  $\lambda = 1, \xi = 1$  and  $m = 2$ . It is depicted from Figure 6a that as  $\lambda$  increases from  $0.70$  to  $15.0$ , both the velocity profiles and the momentum boundary layer thickness decreases. It is particular to note that the velocity profiles become insensitive to

Prandtl number beyond  $Pr = 7.03$ . Also it can be seen from Figure 6b that  $Pr$  has least effect on the temperature profiles as  $Pr$  goes higher than  $7.03$ . Owing to increase in  $Pr$ , both the temperature profiles and the thermal boundary layer thickness decrease.

The effect of increasing value of  $\lambda$  on velocity and temperature profiles for local mixed convection parameter  $\xi = 1, Pr = 7.03$  and  $m = 2$  are presented in Figure 7a and b, respectively. From these Figure, one can observe that as the value of  $\lambda$  increases, there is decrease in the

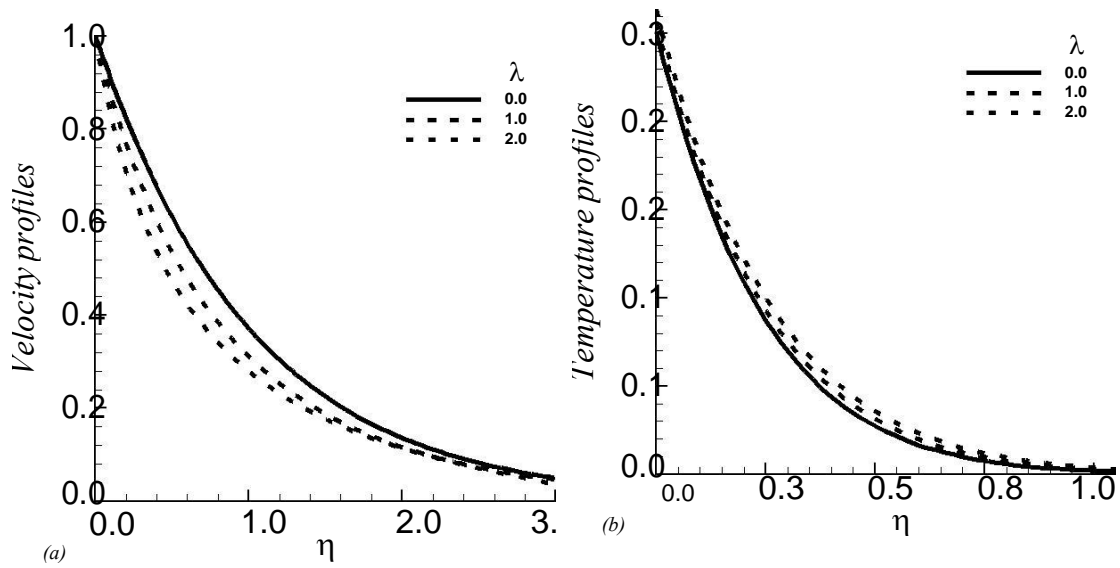


**Figure 7.** Variation of (a) velocity profiles and (b) temperature profiles against  $\eta$  for selected values of the viscoelastic parameter  $\lambda$  when Prandtl number  $Pr = 7.03$ , surface heat flux exponent  $m = 2$  and local mixed convection parameter  $\xi = 1$ .

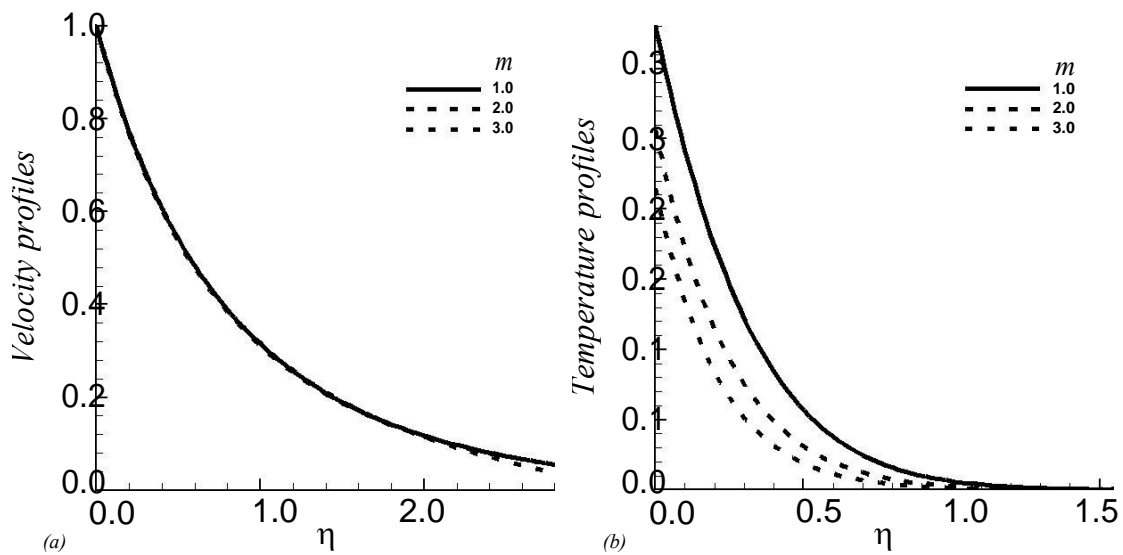


**Figure 8.** Variation of (a) velocity profiles and (b) temperature profiles against  $\eta$  for selected values of surface heat flux exponent  $m$  when Prandtl number  $Pr = 7.03$ , viscoelastic parameter  $\lambda = 1$  and local mixed convection parameter  $\xi = 1$ .

velocity profiles and increase in the temperature profiles in the boundary layer regions and that leads to decrease and increase in the momentum and thermal boundary layer thickness, respectively.

The velocity profiles seems to be have no effect due to increase in  $m$ , while  $Pr = 7.03$ ,  $\lambda$  and  $\xi = 1$  but away from the surface it has effect of decreasing velocity as well as decreasing momentum boundary layer thickness (Figure 8a). From Figure 8b, it is observed that both the

temperature profiles and thermal boundary layer thickness decrease owing to increase in  $m$ .

It is known that when  $\xi = 0$ , the velocity profile corresponds to pure forced convection flow of the second grade fluid along a stretched surface. But with the increase in  $\xi$ , buoyancy force becomes stronger and hence the velocity profile of the fluid increases in the thick region near the surface of the plate. It can further be observed that buoyancy effects tend to disappear away

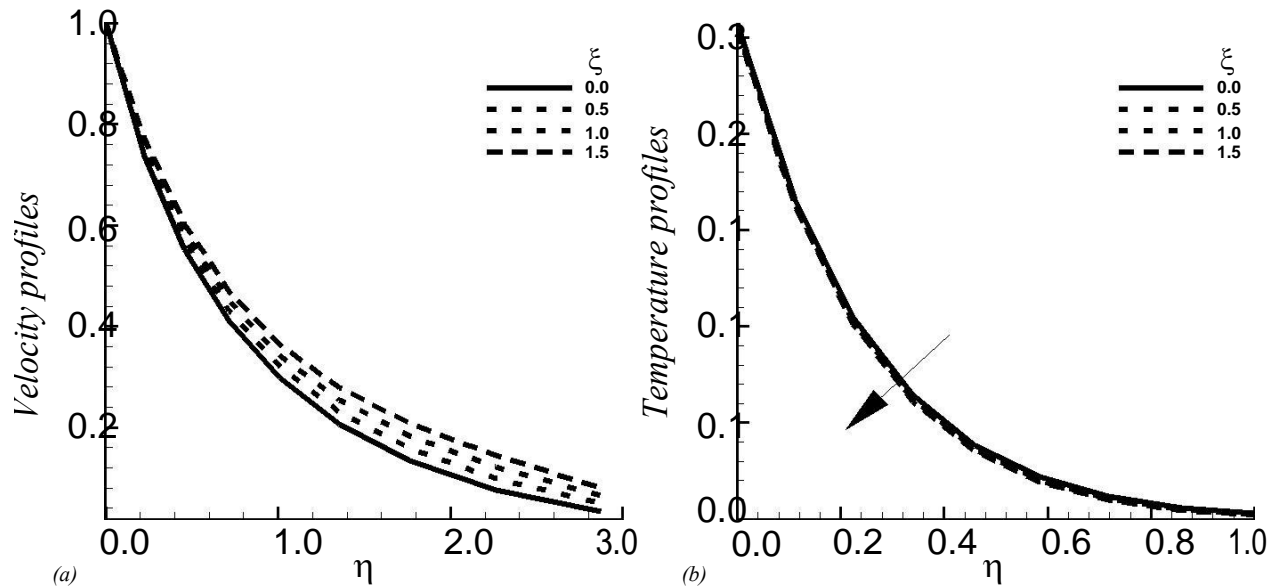


**Figure 9.** Variation of (a) velocity profiles and (b) temperature profiles against  $\eta$  for selected values of local mixed convection parameter  $\xi$  when Prandtl number  $Pr = 7.03$ , viscoelastic parameter  $\lambda = 1$  and surface heat flux exponent  $m = 2$ .

from the surface of the plate (Figure 9a). From Figure 9b, we further see that for  $Pr = 7.03$ ,  $\lambda$  and  $m = 2$ , owing to increase in the mixed convection parameter (local Richardson number),  $\xi$ , temperature profiles decreases whereas the thermal boundary layer thickness seems to be remained the same.

## Conclusions

In the present analysis, we have investigated the mixed convection flow of viscoelastic second grade fluid past a heated and continuously stretched vertical flat plate, numerically. Solutions of the governing equations for momentum and energy for the mixed convection regime have been obtained using two different methods. Here, the numerical results have been provided in terms of the local skin-friction coefficient, local heat transfer coefficient, and velocity and temperature profiles.

From the present investigation, the following conclusions may be drawn:

1. In the mixed convection regime the values of the local skin-friction coefficient and local heat transfer coefficient increase with the increase in  $\xi$ .
2. The values of both the skin-friction coefficient and the heat transfer coefficients decreases near the leading edge owing to increase of  $\lambda$ , and this behavior is reverse in the upstream regime.
3. Increase in the value of  $\lambda$ , leads to decrease the momentum boundary layer thickness and increase in the thermal boundary layer thickness.
4. Owing to increase in  $m$ , both the temperature and

thermal boundary layer thickness decrease whereas no significant change in velocity profiles.

5. Both the momentum and thermal boundary layer thickness are least sensitive to  $\xi$ .

## List of symbols

$C_{fx}$  = local skin friction coefficient  
 $g$  = gravitational acceleration ( $m/sec^2$ )  
 $Gr_x$  = local Grashof number  
 $K$  = kinematic elasticity ( $= \kappa/\rho$ )  
 $Nu_x$  = local Nusselt number  
 $P$  = fluid pressure (Pa)  
 $Pr$  = Prandtl number  
 $q_w$  = heat transfer per unit area at the surface  
 $Re_x$  = local Reynolds number  
 $Ri$  = Richardson number  
 $T$  = temperature ( $^{\circ}C$ )  
 $T_w$  = surface temperature ( $^{\circ}C$ )  
 $T_{\infty}$  = ambient temperature ( $^{\circ}C$ )  
 $U_w$  = velocity of the moving surface (m/s)  
 $u$  = velocity in x-direction (m/s)  
 $v$  = velocity in y-direction (m/s)  
 $U$  = dimensionless velocity in x-direction  
 $V$  = dimensionless velocity in y-direction  
 $x, y$  = Cartesian coordinates (m)  
 $X, Y$  = dimensionless Cartesian coordinates

## Greek symbols

$\alpha$  = thermal diffusivity of the ambient fluid ( $k/\rho c_p$ )

$\beta$  = coefficient of thermal expansion of fluid ( $K^{-1}$ )  
 $\delta$  = momentum boundary layer thickness (m)  
 $\delta_T$  = thermal boundary layer thickness (m)  
 $\eta$  = similarity variable (m)  
 $\theta$  = dimensionless temperature  
 $\kappa$  = second grade parameter  
 $\lambda$  = viscoelastic parameter (Deborah number)  
 $\mu$  = effective dynamic viscosity (Pa/s)  
 $\nu$  = effective kinematic viscosity ( $\mu/\rho$ )  
 $\xi$  = local mixed convection parameter  
 $\rho$  = fluid density at reference temperature  
 $(T_0) \tau_w$  = shear-stress at the surface  
 $\psi$  = stream function ( $m^2/s$ )

## REFERENCES

- Ali M, Al-Yousef F (1998). Laminar mixed convection from a continuously moving vertical surface with suction or injection. *Heat Mass Transf.*, 33: 301-306.
- Altan T, Oh S, Gegel H (1979). *Metal forming fundamentals and applications*, American Society of Metals, Metals Park, OH (Book).
- Bhattacharyya S, Pal A, Gupta AS (1998). Heat transfer in the flow of a viscoelastic fluid over a stretching surface. *Heat Mass Transf.*, 34: 41-45.
- Chen CH (1998). Laminar mixed convection adjacent to vertical, continuously stretching sheets. *Heat Mass Transf.*, 33: 471-476.
- Chen CH (2000). Mixed convection cooling of a heated, continuously stretching surface. *Heat Mass Transf.*, 36: 79-86.
- Chen KC, Char MI, Cleaver JW (1990). Temperature field in non-Newtonian flow over a stretching plate. *J. Math. Anal. Appl.*, 151: 301-307.
- Chen TS (1988). Parabolic systems: Local nonsimilarity method in W. J. Minkowycz et al. (eds.), *Handbook of numerical heat transfer*, Wiley, New York.
- Chen TS, Strobel FA (1980). Buoyancy effects in boundary layer adjacent to a continuous, moving horizontal flat plate. *ASME J. Heat Trans.*, 102: 170-172.
- Dunn JE, Rajagopal KR (1995). Fluids of differential type: Critical review and thermodynamic analysis. *Int. J. Eng. Sci.*, 33: 689-729.
- Fisher EG (1976). *Extrusion of plastics*, Wiley, New York.
- Hossain MA, Banu N, Nakayama A (1994). Non-darcy forced convection boundary layer flow over a wedge embedded in a saturated porous medium, 26: 399-414.
- Hossain MA, Takhar HS (1996). Radiation effect on mixed convection along a vertical plate with uniform temperature. *J. Heat Mass Transf.*, 31: 243-248.
- Ingham DB (1986). Singular and non-unique solutions of the boundary-layer equations for the flow due to free convection near a continuously moving vertical plate. *Appl. Math. Phys.*, (ZAMP) 37: 559-572.
- Kao TT, Domoto GA, Elrod HG (1977). Free convection along a nonisothermal vertical flat plate. *Trans. ASME J. Heat Transf.*, 99: 72-78.
- Karwe MV, Jaluria Y (1988). Fluid flow and mixed convection transport from a moving plate in rolling and extrusion processes. *ASME J. Heat Transf.*, 110: 655-661.
- Karwe MV, Jaluria Y (1991). Numerical simulation of thermal transport associated with a continuously moving flat sheet in materials processing. *ASME J. Heat Transf.*, 113: 612-619.
- Keller HB (1978). Numerical methods in boundary layer theory. *Annu. Rev. Fluid Mech.*, 10: 417-433.
- Keller M, Yang KT (1972). A Görtler-type series for laminar free convection along a non-isothermal vertical flat plate. *Quart. J. Mech. Appl. Math.*, 25: 447-457.
- Liu IC (2005). Flow and heat transfer of an electrically conducting fluid of second grade in a porous medium over a stretching sheet subject to a transverse magnetic field. *Int. J. Non-Linear Mech.*, 40: 465-474.
- Magyari E, Ali ME, Keller B (2001). Heat and mass transfer characteristics of the self-similar boundary-layer flows induced by continuous surface stretched with rapidly decreasing velocities. *Heat Mass Transf.*, 38: 65-74.
- Magyari E, Keller B (2000). Exact solutions for self-similar boundary-layer flows induced by permeable stretching walls. *Eur. J. Mech. B: Fluids*, 19: 109-122.
- Merk HJ (1959). Rapid calculation for boundary-layer transfer using wedge solutions and asymptotic expansions. *J. Fluid Mech.*, 5: 460-480.
- Minkowycz WJ, Sparrow EM (1978). Numerical solution scheme for local nonsimilarity boundary layer analysis. *Numer. Heat Transf.*, 1: 69-85.
- Mushtaq M, Asghar S, Hossain MA (2007). Mixed convection flow of second grade fluid along a vertical stretching flat surface with variable surface temperature. *Heat Mass Transf.*, (in press).
- Rajagopal KR, Na TY, Gupta AS (1984). Flow of a visco-elastic fluid over a stretching sheet. *Rheol. Acta.*, 23: 213-215.
- Sakiadis BC (1961). Boundary layer behavior on continuous solid surfaces: I. boundary-layer equations for two-dimensional and axisymmetric flow. *A.I.Ch.E. J.*, 7(1): 26-28.
- Semenov VI (1984). Similar problems of steady-state laminar free convection on a vertical plate. *Heat Transf. Sov. Res.*, 16: 69-85.
- Sparrow EM, Gregg JL (1958). Similar solutions for free convection from nonisothermal vertical plate. *Trans. ASME J. Heat Transf.*, 80: 379-384.
- Sparrow EM, Quack H, Boerner CJ (1970). Local non-similar boundary layer solutions. *AIAA J.*, 8: 1936-1942.
- Sparrow EM, Yu HS (1971). Local non-similarity thermal boundary layer solutions. *Trans. ASME J. Heat Transf.*, 93: 328-334.
- Tadmor Z, Klein I (1970). *Engineering principles of plasticating extrusion: Polymer Science and Engineering Series*, Van Nostrand Reinhold, New York.
- Walters K (1962). Non-Newtonian effects in some elastico-viscous fluids whose behaviour at small rates of shear is characterised by a general equation of state. *Q. J. Mech. Appl. Math.*, 15: 63-76.
- Yang J, Jeng DR, DeWitt KJ (1982). Laminar free convection from a vertical plate with nonuniform surface conditions. *Numer. Heat Transf.*, 5: 165-184.